# Heterochronic shifts in germband movements contribute to the rapid embryonic development of the coffin fly *Megaselia scalaris*

Karl R. Wotton[1, 2]

[1] EMBL/CRG Systems Biology Research Unit, Centre for Genomic Regulation (CRG), Dr. Aiguader 88, 08003 Barcelona, Spain

[2] Universitat Pompeu Fabra (UPF), Barcelona, Spain

## Abstract

The coffin fly, *Megaselia scalaris,* is a species of medical and forensic importance and is increasingly being used for the study of genetics. Postmortem interval can be estimated based on the life stage of *M. scalaris* recovered from corpses, therefore many studies have addressed the duration of each life stage. These studies demonstrate that embryogenesis completes significantly faster in *M. scalaris* than in the congener *Megaselia abdita* and faster even than the 24 hours needed for *Drosophila melanogaster* embryogenesis. However, until now it has been unclear if this increased speed is achieved by reducing developmental time across all embryonic stages or by the acceleration of individual stages and processes. Here I use time-lapse imaging to create a staging scheme for *M. scalaris* embryogenesis. Comparison of stages between *D. melanogaster* and both *Megaselia* species reveals that heterochronic shifts, simultaneous morphogenetic movements and compression of individual stages all contribute to the rapid development of *M. scalaris*.

## Keywords
Embryology, Megaselia, Development, Diptera, Coffin fly

## Abbreviations
TED: percentage of total embryonic development
AEL: time after egg laying

## 1. Introduction

*Megaselia scalaris* (Loew, 1866) is a fly in the family Phoridae, also referred to as the hump-backed or the scuttle flies. Its ability to reach buried carrion has lead to its use in forensics and is reflected in another alternative name, the coffin fly. This name has the benefit of distinguishing it from *Megaselia abdita*, also referred to as the scuttle fly. In addition to its use in estimating postmortem interval in forsensics, *M. scalaris* is of medical importance due to the ability of its larvae to invade living tissues causing myiasis (see Disney, 2008; Varney and Noor, 2010 for reviews of *M. scalaris* biology).

The genus *Megaselia* forms one of the largest groups among the phorids (one of the earliest branching lineages in the radiation of the cyclorrhaphan flies; see Jiménez-Guri et al., 2013; Wiegmann et al., 2011) and both *M. abdita* and *M. scalaris* have emerged as useful models for genetics. In the case of *M. scalaris,* this has mostly focused on sex determination (Sievert et al., 1997; Traut, 2010, 1994; Willhoeft and Traut, 1995, 1990), while the focus with *M. abdita* has been on embryonic development (Lemke et al., 2008; Rafiqi et al., 2008; Stauber et al., 2008, 2000, 1999; Wotton et al., 2014).

Genomic resources exist for both species, with a transcriptome available for *M. abdita* (Jiménez-Guri et al., 2013; http://diptex.crg.es/) and a genome available for *M. scalaris* (Rasmussen and Noor, 2009; http://metazoa.ensembl.org/Megaselia_scalaris). Additionally, techniques developed for *M. abdita*, including in situ hybridisation (Crombach et al., 2012a, 2012b; Wotton et al., 2014) and gene knock-down (Rafiqi et al., 2011a, 2011b, 2011c) are likely to be directly applicable to *M. scalaris*.

Numerous publications have addressed the duration of *M. scalaris* development at different temperatures (see Table 1 in Disney, 2008) with egg to adult taking 17.2-

18.4 days at 25°C, of which around 17 hours were needed for embryonic development (Prawirodisastro and Benjamin, 1979). Embryonic development in *M. abdita* (Sander strain; see Rafiqi et al., 2011d) lasts significantly longer than this, at least 24 hours (as in *D. Melanogaster*) and up to around 27.5 hours under oil (Rafiqi et al., 2011a; Wotton et al., 2014). However, no systematic characterisation and analysis of *M. scalaris* embryonic development has been carried out. To investigate whether this reduced developmental time is the result of a global decrease in developmental time at each embryonic stage or a reduction in individual stages or events, I carried out a detailed description of embryonic development. Stages were homologised to *D. melanogaster* and *M. abdita* development. Comparison of stages across all 3 species reveals a number of features that contribute to the rapid embryonic development of *M. scalaris*.

## 2. Materials and Methods

### 2.1 Fly culture and embryo collection

*M. scalaris* were sourced from the lab of Pat Simpson (University of Cambridge, UK). Embryos were collected after 5–10 minutes (min) laying time, and dechorionated for 1 min 20 seconds in 25% bleach (sodium hypochlorite 10%, Sigma-Aldrich; 2.5% active sodium hypochlorite). To image the embryos I brushed the dechorionated embryos onto a microscopy slide and covered them with a drop of 10S Voltalef oil ensuring that the embryos did not dry out.

### 2.2 Time-lapse imaging

Slides were placed on a temperature-controlled platform at 25°C, and embryos were imaged with a Leica DM6000B upright compound microscope using a 20x objective, and time intervals between image acquisitions of every 1 min. Specifications of

embryo orientation for each time-lapse are provided in Supporting File S1. Movies were processed using ImageJ (http://rsbweb.nih.gov/ij).

## 3. Results & Discussion

### 3.1 Embryonic staging scheme for *M. scalaris* development

Embryos were collected shortly after egg laying, dechorinated and placed on a microscope slide under Voltalef oil. Live imaging with differential interference contrast (DIC) was used to produce a series of movies covering all stages of embryonic development (see Supporting Movie S1). At 25°C and under Voltalef oil embryogenesis lasts approximately 22 hours (hrs) from oviposition until hatching, 2 hours shorter than in *D. melanogaster* and approximately 5 hrs 30 min shorter than in the congener *M. abdita*.

Development can be divided into 17 stages roughly corresponding to Bownes' stages in *D. melanogaster* and *M. abdita* (Campos-Ortega and Hartenstein, 1997; Wotton et al., 2014). Each stage can be distinguished by distinct morphological markers, as shown in Figure 1 (also see Supporting Movie S1). The similarity between *D. melanogaster, M. abdita* and *M. scalaris* development allows a direct comparison between developmental stages, as discussed below and shown in Table 1 and Figure 2 (see section 3.2).

In this section, I provide an overview over all stages of development and provide a comparison to the well characterised embryology of *D. melanogaster* (Campos-Ortega and Hartenstein, 1997). All times are displayed as hrs:min unless otherwise indicated. Raw data for each event including the number of embryos examined *(n)* and standard deviations (SDs) are supplied in Supporting File S1. Measurements were taken from 4 individuals; standard deviation is generally below 10 minutes but increases around the hatching stage (see Supporting File S1). To assist identification

of stages under different conditions (i.e. not under oil), and at different temperatures, a percentage of total embryonic development (TED) is supplied.
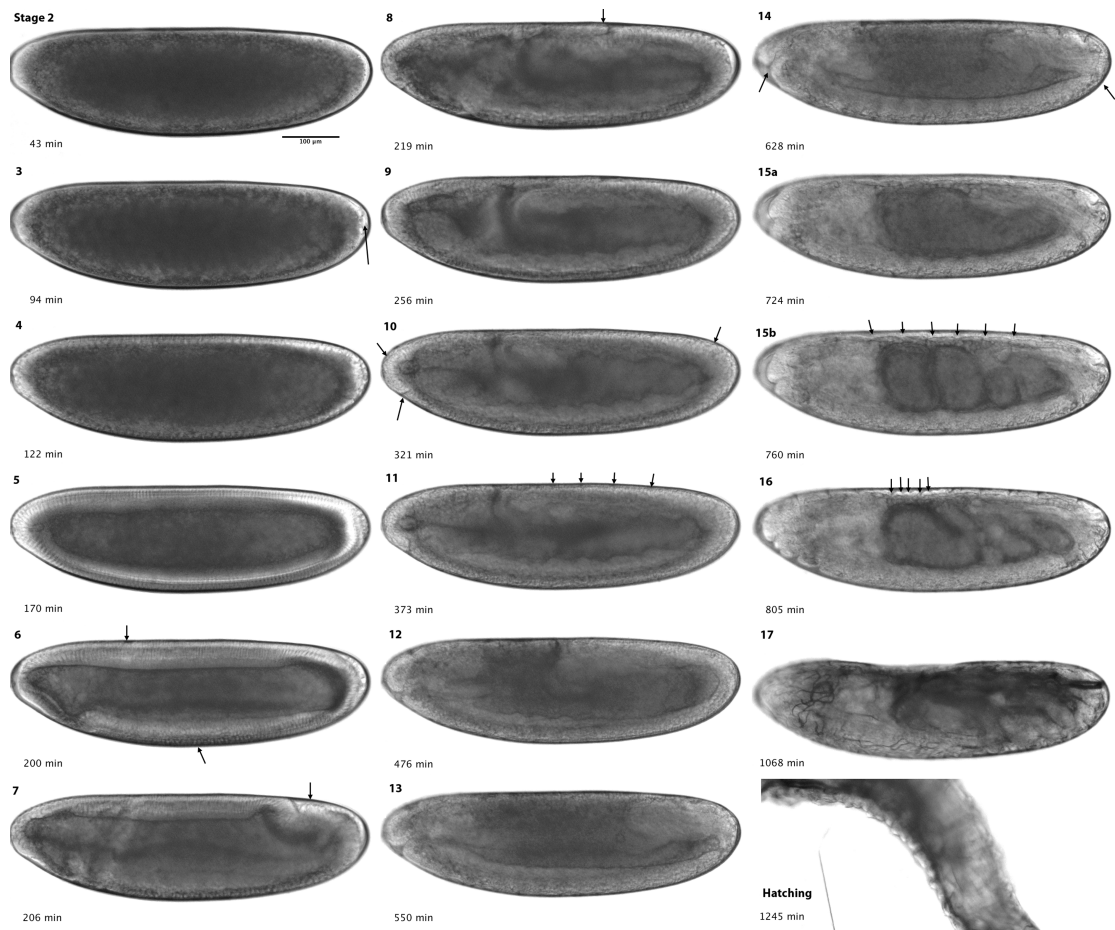


**Figure 1. Embryonic staging and developmental events in *M. scalaris.*** Embryos are shown as lateral views: anterior is to the left, dorsal is up. Stage numbers (roughly corresponding to Bownes' stages in *D. melanogaster*) are shown at the top left, and time after egg laying (AEL) in minutes in the bottom left corner of each panel. Black arrows indicate morphological landmarks. See main text for a detailed description, and Figure 2 and Table 1 for comparative timing of stages with reference to *D. melanogaster* and *M. abdita*.

*Stage 1:* 0:00–0:20 (duration: 0:20, 1.5% TED). This stage begins at egg laying and includes the first two cleavage divisions. The number of cleavage cycles appears to be conserved within the Diptera with *D. melanogaster*, *M. abdita* and *C. albipunctata* all undergoing 14 cleavage cycles before gastrulation (Foe and Alberts, 1983;

Jiménez-Guri et al., 2014), I therefore base the timings for *M. scalaris* development on this observation.  Since all cleavage cycles up to C12 are of a very similar duration (approximately 10 min), we infer stage 1 to last for at least 20 min. All 'times after egg laying (AEL)' below include a correction based on this estimate (see Supporting File S1 for raw timing data, and time adjustment values). In *D. melanogaster*, stage 1 occurs over a 25 min period (1.4% TED) (Campos-Ortega and Hartenstein, 1997 and references to *D. melanogaster* development hereafter unless stated).

*Stage 2:* 0:20–1:28 (duration: 1:08, 5.2% TED). Cleavage cycles C3 to C8 take place. During this time, an empty space appears between the vitelline membrane and the egg cytoplasm at the anterior and posterior poles. In *D. melanogaster*, stage 2 occurs from 0:25–1:05 and takes 0:40 (3% TED).

*Stage 3:* 1:28–1:38 (duration: 0:10, 0.8% TED). This stage includes cleavage cycle C9 and the beginning of C10. At this stage, nuclei divide and migrate outwards, and the pole buds form (Figure 1, stage 3, black arrow). In *D. melanogaster*, this stage occurs from 1:05–1:20 and lasts for 0:15 (1% TED). During this stage, the empty space at the posterior of the embryo disappears in both species. Cleavage divisions during the blastoderm stages can be detected by the disappearance of nuclear envelopes, and their subsequent reappearance at the beginning of the interphase of each cycle. The duration of blastoderm cleavage cycle 10 for *D. melanogaster*, *M. abdita* and *M. scalaris* is around 9, 13 and 13 min respectively.

*Stage 4:* 1:38–2:39 (duration: 0:61, 4.7% TED). At the onset of this stage, the nuclei have reached the periphery and form the syncytial blastoderm, cleavage cycles 11 to 13 take place. In *D. melanogaster*, the syncytial blastoderm stage occurs from 1:20–2:10 and lasts for 0:50 (3.5% TED). The durations of blastoderm cleavage cycles 11-

13 for *D. melanogaster*, are around 10, 12 and 21 min, for *M. abdita*: 11, 14 and 23 min, and for *M. scalaris*: 12, 12 and 20 min respectively.

***Stage 5:*** 2:39–3:19 (duration: 0:40, 3% TED). Similar to previous blastoderm cycles, cellular membranes begin to form at cleavage cycle C14, but these now progressively grow to engulf the elongating blastoderm nuclei forming the cellular blastoderm. Nuclear morphology changes from circular to elongated. In *D. melanogaster*, this stage occurs from 2:10–2:50 and lasts for 0:40 (3% TED).

***Stage 6:*** 3:19–3:27 (duration: 0:08, 0.6% TED). This stage begins at the onset of gastrulation, and is marked by the wavy appearance of the ventral blastoderm cells (seen as uneven apical and basal surfaces), and the slight dorsal movement of the pole cells. During this stage early gastrulation events occur: the ventral and cephalic furrows form (Figure 1, stage 6, black arrows), and the pole cells continue to shift dorsally. In *D. melanogaster*, this stage occurs from 2:50–3:00 and lasts for 0:10 (1% TED).

***Stage 7:*** 3:27–3:32 (duration: 0:05, 0.4% TED). This stage begins with the pole cell plate in a horizontal position (parallel to the A–P axis; Figure 1, stage 7, black arrow). The plate continues to tilt, forming a pocket (the amnioproctodeal invagination). The dorsal folds and amnioproctodeal invagination are less conspicuous in both *M. scalaris* and *M. abdita* movies. In *D. melanogaster*, this stage occurs from 3:00–3:10 and lasts for 0:10 (1% TED).

***Stage 8:*** 3:32–4:39 (duration: 1:07, 5.1% TED). This stage starts with the cephalad (headwards) movement of the amnioproctodeal invagination, marking the onset of the rapid phase of germband extension. The germband reaches approximately 40% A–P position (0% A–P position is at the anterior pole) from a starting point of approximately 80% A–P position, and the amnioserosal lip forms (Figure 1, stage 8, black arrow). Beginning from this lip, the serosa expands to eventually engulf the

entire embryo at stage 11 as is also is seen in *M. abdita.* Interestingly this stage lasts

longer in both *Megaselia* species than in *D. melanogaster*. In *D. melanogaster*, this

stage occurs from 3:10–3:40 and lasts for 0:30 (2% TED). During this time, the

germband reaches beyond 40% A–P position. On the other hand, no serosal

expansion occurs in *D. melanogaster* since extraembryonic tissues are reduced to a

dorsal amnioserosa.

*Stage 9:* 4:39–5:07 (duration: 0:28, 2.1% TED). This stage commences with the

transient appearance of mesodermal segmentation. The germband continues to

extend but at a slower rate (slow phase of germband extension), and the serosa

continues to migrate ventrally. Also at this stage, and unlike in *D. melanogaster* and

*M. abdita* where it occurs at stage 10*,* the germband reaches its maximum extent,

around 30% A–P position. In *D. melanogaster*, this stage occurs from 3:40–4:20 and

lasts for 0:40 (3% TED).

*Stage 10:* 5:07–6:05 (duration: 0:58, 4.4% TED) This stage commences with the

formation of the stomodeum (Figure 1, stage 10, ventral-anterior black arrow). During

this time, the serosa continues to migrate (Figure 1, stage 10, dorso-lateral black

arrows). In *D. melanogaster*, this stage occurs from 4:20–5:20 and lasts for 1:00 (4%

TED), during which the germband reaches its maximum extent at 25% A–P position.

*Stage 11:* 6:05–6:48 (duration: 0:43, 3.3% TED). This stage begins with the

appearance of parasegmental furrows (Figure 1, stage 11, dorsal black arrows).

During this time the serosa fuses forming a complete extraembryonic layer around

the embryo. The serosa remains intact for around 4.5 hrs before finally breaking at

stage 14. In contrast, this extraembryonic layer persists for around 7 hrs in *M. abdita*

and consequently does not break until stage 15. In *D. melanogaster*, this stage

occurs from 5:20–7:20 and lasts for 2:00 (8% TED).

*Stage 12:* 6:48–8:54 (duration: 2:06, 9.6% TED). The onset of this stage is marked by the beginning of germband retraction. In *D. melanogaster*, this stage occurs from 7:20–9:20 and lasts for 2:00 (8% TED).

*Stage 13:* 8:54–9:18 (duration: 0:24, 1.8% TED). This stage begins with the completion of germband retraction. During this time, the dorsal opening of the embryo remains covered by the amnion, and the serosa envelopes the entire embryo. Dorsal closure starts at the same time as the lengthening of the gut. In *D. melanogaster*, this stage occurs from 9:20–10:20 and lasts for 1:00 (4% TED), during which the dorsal egg surface remains open and the dorsal hole is covered by the amnioserosa.

*Stage 14:* 9:18–11:08 (duration: 1:50, 8.4% TED). This stage starts at the beginning of head involution. During this time, the serosa ruptures (10:40) at a ventro-posterior position, slightly more pole-ward than in *M. abdita* and one stage earlier (Figure 1, stage 14, black arrow at posterior pole). During its retraction, the serosa first rounds the posterior pole before rounding the anterior pole, to be contracted into the dorsal hole 40 min after rupturing (retraction also takes 40 min in *M. abdita*). Additionally during this stage, the ventral nerve cord (VNC) starts to shorten. In contrast, this occurs during stage 15 in *M. abdita* and at stage 16 in *D. melanogaster*. The head continues to involute beyond the end of this stage (Figure 1, stage 14, black arrow at anterior pole), and this process completes only by the time the serosa ruptures at stage 15. In *D. melanogaster*, stage 14 occurs from 10:20–11:20 and lasts for 1:00 (1.4% TED).

*Stage 15:* 11:08–13:25 (duration: 2:17, 10.4% TED). This stage starts at the closure of the midgut (Figure 1, stage 15a), dorsal closure completes and dorsal epidermal segmentation is visible (Figure 1, stage 15b, black arrows). Following these events three constrictions form in the midgut, almost simultaneously, subdividing it into four

chambers. In contrast, in *D. melanogaster* and *M. abdita,* these gut constrictions emerge individually over an approximately 30 minute window. By the end of stage 15 these chambers have become obscured by further constrictions in *M. scalaris* but persist into stage 16 in the other species. Also during this stage muscle contractions begin. In *D. melanogaster*, this stage occurs from 11:20–13:00 and lasts for 1:40 (7% TED).

*Stage 16:* 13.25–13:44 (duration: 0:19, 1.5% TED). This stage begins with the appearance of the intersegmental grooves at mid-dorsal levels (Figure 1, stage 16, black arrows). In *M abdita* the midgut remains visible as 4 chambers for a short time, while this division persists for significantly longer in *D. melanogaster.* The divisions of the midgut, although originating during stage 15, are often used to characterise *D. melanogaster* stage 16 embryos (Hartenstein, 1993). The lack of this morphological feature in *M. scalaris,* and its short persistence in *M. abidta,* make this feature unsuitable as a stage 16 marker in these species. Also during this stage the VNC continues to shorten; completion of this movement is not clearly detectable and probably continues into stage 17. In *D. melanogaster*, this stage occurs from 13:00–16:00 and lasts for 3:00 (13% TED).

*Stage 17:* 13:44–21:53 (duration: 8:09, 37% TED). This stage commences when the dorsal ridge has completely overgrown the tip of the clypeolabrum (completion of head involution). During this stage, the retraction of the VNC is likely to continue and reach completion. The trachea fill with air at around 18 hrs AEL. The first instar larva hatches at around 22 hrs AEL. In *D. melanogaster*, this stage occurs from 16:00–24:00 and lasts for 8:00 hrs (33% TED).

## 3.2 Comparative analysis of embryonic development in *M. scalaris, M. abdita* and *D. melanogaster*

*M. scalaris* embryonic development completes approximately 2 hrs faster than in *D. melanogaster* and 5.5 hrs faster than in the congener *M. abdita*. A comparative overview of embryonic development between *D. melanogaster, M. abdita* and *M. scalaris* is shown in Figure 2, while stage durations and %TED values are shown in Table 1. Using these resources I next discuss the features of *M. scalaris* that may account for the decreased time needed for embryonic development.

The timings of stages 1 to 7 are remarkably similar in all 3 species. At the start of stage 7 (when the pole cell plate reaches a horizontal position) only 30 min separates *D. melanogaster* (at 3 hrs AEL) from *M. scalaris,* and 45 min from *D. melanogaster* to *M. abdita*.

At stage 8 serosal migration begins in both *Megaselia* species but is absent from *D. melanogaster*. As this stage lacks heterochronies and is consistently longer in both *Megaselia* species (40 min longer in *M. scalaris* and 1 hr 10 min longer in *M. abdita*) it is tempting to speculate that this stage is lengthened to accommodate these movements.

At stage 9 the germband of *M. scalaris* reaches its maximum extent, one stage earlier than in the other species (Campos-Ortega and Hartenstein, 1997; Wotton et al., 2014). This represents a large heterochronic shift and consequently the time at which the germband retracts (at stage 12) starts around 1 hr 20 min before it occurs in *M. abdita*. Additionally, germband retraction is completed as quickly in *M. scalaris* as in *D. melanogaster*, around 50 min quicker than in *M. abdita*. These features of germband extension create a relatively short stage 11 (30 min shorter than in *M. abdita* and 1 hr 17 min shorter than in *D. melanogaster*) and consequently *M. scalaris* reaches the end of stage 11 before *D. melanogaster*. Stage 12 lasts for around 2 hrs

in both *D. melanogaster* and *M. scalaris* but continues for an additional 50 min in *M. abdita*. At the stage 13/14 boundary, in *M. scalaris,* dorsal closure and head involution occur simultaneously (in *M. abdita*, the start of head involution occurs approximately 1 hour after dorsal closure begins) and this, together with the altered germband dynamics, forms a shorter stage 13 than in the other species. Therefore *M. scalaris* remains ahead in development until the end of stage 13.

A further heterochronic shift in *M. scalaris* sees the shortening of the VNS beginning at stage 14, a stage earlier than in *M. abdita* (stage 15), and 2 stages earlier than in *D. melanogaster* (stage 16). Additionally, at this stage the serosa ruptures and is contracted into the dorsal hole one stage earlier than in *M. abdita*. The disappearance of the serosa is correlated with a lengthened stage 14 in *M. scalaris* (50 min more than in *D. melanogaster* and 34 min more than in *M. abdita*) and a lengthened stage 15 in *M. abdita*.

Stage 16 is significantly shorter in both *Megaselia* species than in *D. melanogaster* (2 hrs 40 min shorter in *M. scalaris*) and allows *M. scalaris* to begin stage 17 around 2 hrs 16 min before *D. melanogaster,* and around 4 hrs before *M. abdita* starts. Additionally, during stage 16, and unlike in the other species, midgut constrictions occur almost simultaneously and do not persist into stage 17, suggesting that midgut development proceeds faster in this species.  Finally, stage 17 ends embryonic development and takes around 8 hrs in both *M. scalaris* and *D. melanogaster* while *M. abdita* requires a further 2 hrs before hatching.
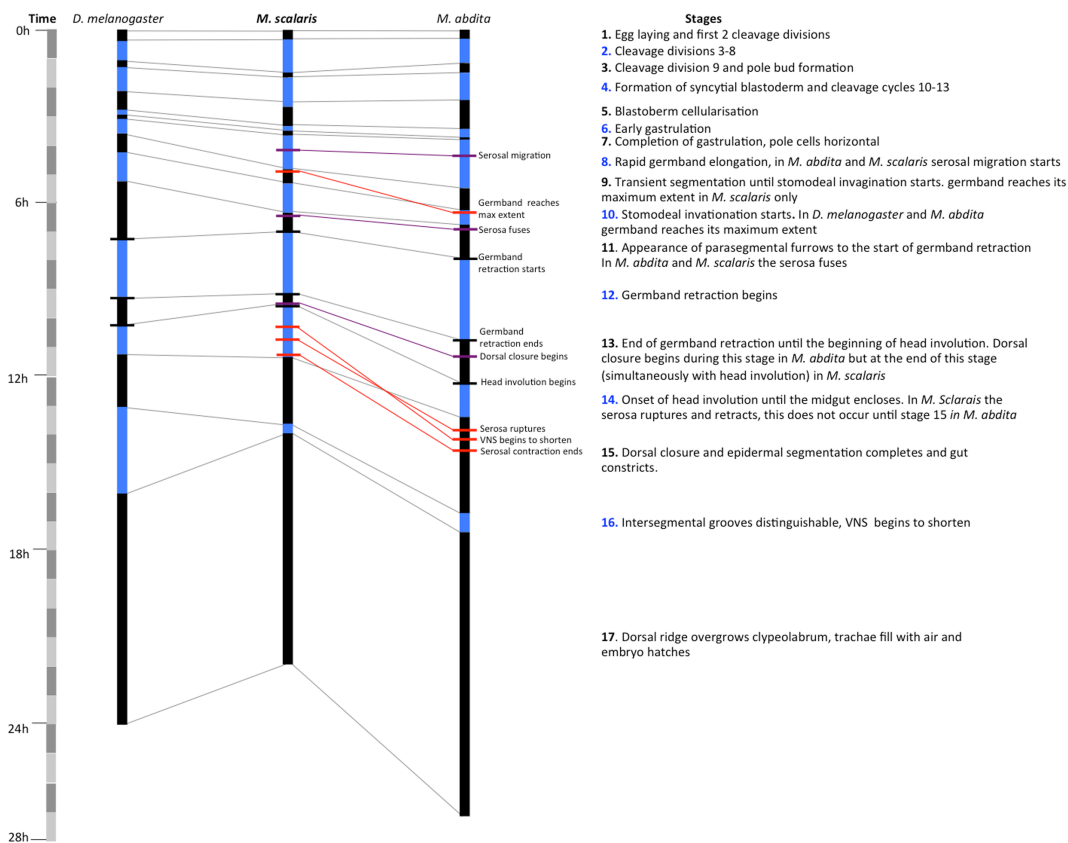
**Stages**

1. Egg laying and first 2 cleavage divisions
2. Cleavage divisions 3-8
3. Cleavage division 9 and pole bud formation
4. Formation of syncytial blastoderm and cleavage cycles 10-13

5. Blastoberm cellularisation
6. Early gastrulation
7. Completion of gastrulation, pole cells horizontal
8. Rapid germband elongation, in *M. abdita* and *M. scalaris* serosal migration starts
9. Transient segmentation until stomodeal invagination starts. germband reaches its maximum extent in *M. scalaris* only
10. Stomodeal invagination starts. In *D. melanogaster* and *M. abdita* germband reaches its maximum extent
11. Appearance of parasegmental furrows to the start of germband retraction In *M. abdita* and *M. scalaris* the serosa fuses

12. Germband retraction begins

13. End of germband retraction until the beginning of head involution. Dorsal closure begins during this stage in *M. abdita* but at the end of this stage (simultaneously with head involution) in *M. scalaris*

14. Onset of head involution until the midgut encloses. In *M. Sclaraïs* the serosa ruptures and retracts, this does not occur until stage 15 *in M. abdita*

15. Dorsal closure and epidermal segmentation completes and gut constricts.

16. Intersegmental grooves distinguishable, VNS begins to shorten

17. Dorsal ridge overgrows clypeolabrum, trachae fill with air and embryo hatches

Landmarks (on figure): Serosal migration; Germband reaches max extent; Serosa fuses; Germband retraction starts; Germband retraction ends; Dorsal closure begins; Head involution begins; Serosa ruptures; VNS begins to shorten; Serosal contraction ends

Time axis: 0h, 6h, 12h, 18h, 24h, 28h

Columns: *D. melanogaster*, **M. scalaris**, *M. abdita*

**Figure 2. Comparative timing of embryonic developmental stages in *D. melanogaster, M. scalaris* and *M. abdita*.** The duration of each stage is shown for each species in alternating black and blue bars. The time scale is divided into blocks of 1 hr on the far left hand side. A brief description of each stage is given on the right. Landmarks of development are indicated to the right of the *M. abdita* time scale and discussed in the text. Red horizontal bars indicate heterochronic shifts between *M. abdita* and *M. scalaris*, purple bars indicate landmark events occurring during a stage, while black bars indicate landmark events occurring at stage boundaries.

| Stage | D. melanogaster (Campos-Ortega and Hartenstein, 1997) Stage duration | %TED | M. abdita (Wotton et al., 2014) Stage duration | %TED | M. scalaris Stage duration | %TED |
|---|---|---|---|---|---|---|
| 1 | 0:25 | 1.4 | 0:20 | 1.2 | 0:20 | 1.5 |
| 2 | 0:40 | 3 | 0:50 | 3 | 1:08 | 5.2 |
| 3 | 0:15 | 1 | 0:23 | 1.4 | 0:10 | 0.8 |
| 4 | 0:50 | 3.5 | 0:57 | 3.4 | 1:01 | 4.7 |
| 5 | 0:40 | 3 | 0:58 | 4 | 0:40 | 3.0 |
| 6 | 0:10 | 1 | 0:18 | 1 | 0:08 | 0.6 |
| 7 | 0:10 | 1 | 0:05 | 0.3 | 0:05 | 0.4 |
| 8 | 0:30 | 2 | 1:38 | 6 | 1:07 | 5.1 |
| 9 | 0:40 | 3 | 0:47 | 3 | 0:28 | 2.1 |
| 10 | 1:00 | 4 | 0:33 | 2 | 0:58 | 4.4 |
| 11 | 2:00 | 8 | 1:13 | 4 | 0:43 | 3.3 |
| 12 | 2:00 | 8 | 2:51 | 10 | 2:06 | 9.6 |
| 13 | 1:00 | 4 | 1:26 | 5.2 | 0:24 | 1.8 |
| 14 | 1:00 | 4 | 1:14 | 4 | 1:50 | 8.4 |
| 15 | 1:40 | 7 | 3:20 | 12 | 2:17 | 10.4 |
| 16 | 3:00 | 13 | 0:42 | 3 | 0:19 | 1.5 |
| 17 | 8:00 | 33 | 9:54 | 36 | 8:09 | 37.2 |
| Total | 24:00 | 100 | 27:36 | 100 | 21:53 | 100.0 |

**Table 1.** Stage durations in hours and minutes along with %TED values for stages 1 to 17 of embryonic development in *D. melanogaster, M. abdita* and *M. scalaris.*

Comparison of embryonic stages and developmental events across the 3 species indicates a number of features that contribute to the decreased developmental time needed to go from egg to larva *in M. scalaris*. First, I find that the germband reaches its maximum extent a stage earlier than in the other species and a consequence of this heterochronic shift is that the germband is able to retract sooner. Second, I find simultaneous movements of head involution and dorsal closure that are not present in *M. abdita.* These two differences result in a compression of the time need to progress through stages 9 to 13. Third, I find a significantly compressed stage 16 in both *Megselia* species, again decreasing the developmental time of *M. scalaris* over *D. melanogaster*. The fourth feature is a heterochronic shift in the stage at which the serosa ruptures and contracts, this results in a reduction of the time during which *M.*

*scalaris* is enclosed in extraembryonic membrane. The fifth feature is a heterochronic shift in the timing at which the ventral nervous system begins to shorten, from stage 16 in *D. melanogaster* and stage 15 in *M. abdita* to stage 14 *in M. scalaris*. Finally, the sixth feature combines simultaneous constrictions of the midgut with rapid midgut development. This results in a heterochronic shift in the resolution of the four midgut chambers, such that they become obscured by further constrictions before the end of stage 15 rather than during stage 16.

## 4. Conclusions

In this paper I provide a detailed description of the embryonic development of the coffin fly *M. scalaris.* In agreement with previous results, *M. scalaris* embryogenesis is found to require less time to complete than *D. melanogaster,* and significantly less time than the congener *M. abdita*. Comparison of stages across all 3 species reveals that heterochronic shifts, simultaneous morphogenetic movements and compression of individual stages all contribute to this rapid development.

## Acknowledgments

## Supplementary Figures

**Supporting Movie S1. Time-lapse movie of *M. scalaris* development**

Time-lapse movie of a *M. scalaris* embryo taken using a 20x objective and DIC optics under 10S Voltalef oil. This movie corresponds to time-lapse 3 in Supporting File S1.

**Supporting File S1. Timing of developmental events from individual time-lapse movies in *M. scalaris.***

Stages and developmental events are shown in columns A, B, AC and AD. The green-headed columns and the blue-headed columns indicate developmental timing for *D. melanogaster* (Campos-Ortega and Hartenstein, 1997) and *M. abdita* (Wotton et al., 2014) respectively. Orange headed columns indicate *M. scalaris* data. Time-lapse IDs are listed along the top along with averages in minutes, hours and minutes (h:m). Also listed are n numbers for each event, stage duration (in minutes and in h:m) and standard deviation (STDEV) for each event. % of developmental time is show for each stage (%TED). Raw data for time-lapses 1-4 are shown in columns L-O along with details of embryo orientation, optics and time intervals used. Columns Q-T show the same time-lapses after a time adjustment has been made. In brief, 10 minutes is added for each unrecorded cleavage cycle (i.e time-lapse 4 starts at 11min in the raw data, therefore the start of the movie is C3 + 9min. By adding 9 min we arrive at the start of C3, by adding another 10 min we arrive at the start of C2, and adding another 10min the start of C1. Hence, to normalise this movie I add 9+10+10= 29min). Alternating white and grey rows mark events occurring within a stage. Stages marked in blue indicate heterochronic shifts in developmental events.

# References

Campos-Ortega, J., Hartenstein, V., 1997. The Embryonic Development of Drosophila melanogaster (2nd Edition), Springer, Heidelberg, DE. Springer, Heidelberg, DE.

Crombach, A., Wotton, K.R., Cicin-Sain, D., Ashyraliyev, M., Jaeger, J., 2012a. Efficient Reverse-Engineering of a Developmental Gene Regulatory Network. PLoS Comput. Biol. 8, e1002589.

Crombach, A., Wotton, K.R., Cicin-Sain, D., Jaeger, J., 2012b. Medium-Throughput Processing of Whole Mount In Situ Hybridisation Experiments into Gene Expression Domains. PLoS One 7, e46658.

Disney, R.H.L., 2008. Natural history of the scuttle fly, Megaselia scalaris. Annu. Rev. Entomol. 53, 39–60.

Foe, V.E., Alberts, B.M., 1983. Studies of nuclear and cytoplasmic behaviour during the five mitotic cycles that precede gastrulation in Drosophila embryogenesis. J. Cell Sci. 61, 31–70.

Hartenstein, V., 1993. Atlas of Drosophila Development. Cold Spring Harbor Laboratory Press.

Jiménez-Guri, E., Huerta-Cepas, J., Cozzuto, L., Wotton, K.R., Kang, H., Himmelbauer, H., Roma, G., Gabaldón, T., Jaeger, J., 2013. Comparative transcriptomics of early dipteran development. BMC Genomics 14, 123.

Jiménez-Guri, E., Wotton, K.R., Gavilán, B., Jaeger, J., Jimenez-Guri, E., 2014. A staging scheme for the development of the moth midge Clogmia albipunctata. PLoS One 9, e84422.

Lemke, S., Stauber, M., Shaw, P.J., Rafiqi, A.M., Prell, A., Schmidt-Ott, U., 2008. Bicoid occurrence and Bicoid-dependent hunchback regulation in lower cyclorrhaphan flies. Evol. Dev. 10, 413–20.

Prawirodisastro, M., Benjamin, D., 1979. Laboratory study of the biology and ecology of Megaselia scalaris (Diptera, Phoridae). J. Med. Entomol. 16, 317–20.

Rafiqi, A., Lemke, S., Schmidt-Ott, U., 2011a. Megaselia abdita : Cuticle Preparation from Injected Embryos. Cold Spring Harb. Protoc. 4, 432–434.

Rafiqi, A., Lemke, S., Schmidt-Ott, U., 2011b. Megaselia abdita: Fixing and Devitellinizing Embryos Protocol. Cold Spring Harb. Protoc. 4, 429–431.

Rafiqi, A., Lemke, S., Schmidt-Ott, U., 2011c. Megaselia abdita: Preparing Embryos for Injection. Cold Spring Harb. Protoc. 4, 426–428.

Rafiqi, A., Lemke, S., Schmidt-Ott, U., 2011d. The Scuttle Fly Megaselia abdita (Phoridae): A Link between Drosophila and Mosquito Development. Cold Spring Harb. Protoc. 4, 349–353.

Rafiqi, A.M., Lemke, S., Ferguson, S., Stauber, M., Schmidt-Ott, U., 2008. Evolutionary origin of the amnioserosa in cyclorrhaphan flies correlates with spatial and temporal expression changes of zen. Proc. Natl. Acad. Sci. U. S. A. 105, 234–9.

Rasmussen, D.A., Noor, M.A.F., 2009. What can you do with 0.1x genome coverage? A case study based on a genome survey of the scuttle fly Megaselia scalaris (Phoridae). BMC Genomics 10, 382.

Sievert, V., Kuhn, S., Traut, W., 1997. Expression of the sex determining cascade genes Sex-lethal and doublesex in the phorid fly Megaselia scalaris. Genome 40, 211–214.

Stauber, M., Jäckle, H., Schmidt-Ott, U., 1999. The anterior determinant bicoid of Drosophila is a derived Hox class 3 gene. Proc. Natl. Acad. Sci. U. S. A. 96, 3786–9.

Stauber, M., Lemke, S., Schmidt-Ott, U., 2008. Expression and regulation of caudal in the lower cyclorrhaphan fly Megaselia. Dev. Genes Evol. 218, 81–7.

Stauber, M., Taubert, H., Schmidt-Ott, U., 2000. Function of bicoid and hunchback homologs in the basal cyclorrhaphan fly Megaselia (Phoridae). Proc. Natl. Acad. Sci. U. S. A. 97, 10844–9.

Traut, W., 1994. Sex determination in the fly Megaselia scalaris, a model system for primary steps of sex chromosome evolution. Genetics 136, 1097–1104.

Traut, W., 2010. New Y chromosomes and early stages of sex chromosome differentiation: sex determination in Megaselia. J. Genet. 89, 307–313.

Varney, R., Noor, M., 2010. The scuttle fly. Curr. Biol. 20, 466–467.

Wiegmann, B.M., Trautwein, M.D., Winkler, I.S., Barr, N.B., Kim, J.-W., Lambkin, C., Bertone, M. a, Cassel, B.K., Bayless, K.M., Heimberg, A.M., Wheeler, B.M., Peterson, K.J., Pape, T., Sinclair, B.J., Skevington, J.H., Blagoderov, V., Caravas, J., Kutty, S.N., Schmidt-Ott, U., Kampmeier, G.E., Thompson, F.C., Grimaldi, D.A., Beckenbach, A.T., Courtney, G.W., Friedrich, M., Meier, R., Yeates, D.K., 2011. Episodic radiations in the fly tree of life. Proc. Natl. Acad. Sci. U. S. A. 108, 5690–5.

Willhoeft, U., Traut, W., 1990. Molecular differentiation of the homomorphic sex chromosomes in Megaselia scalaris (Diptera) detected by random DNA probes. Chromosoma 99, 237–242.

Willhoeft, U., Traut, W., 1995. The sex-determining region of the Megaselia scalaris (Diptera) Y chromosome. Chromosome Res. 3, 59–65.

Wotton, K.R., Jiménez-Guri, E., García Matheu, B., Jaeger, J., 2014. A Staging Scheme for the Development of the Scuttle Fly Megaselia abdita. PLoS One 9, e84421.